Estimation of Baseline Drifts in fMRI

François G. Meyer[1]* and Gregory McCarthy[2]

[1] Department of Electrical Engineering, University of Colorado at Boulder
Department of Radiology, University of Colorado Health Sciences Center
francois.meyer@colorado.edu
[2] Brain Imaging and Analysis Center, Box 3808
Duke University Medical Center, Durham, NC 27710

Abstract. This work provides a new method to estimate and remove baseline drifts in the fMRI signal. The baseline drift in each time series is described as a superposition of physical and physiological phenomena that occur at different scales. A fast algorithm, based on a wavelet representation of the data yields detrended time-series. Experiments with fMRI data demonstrate that our detrending technique can infer and remove drifts that cannot be adequately represented with low degree polynomials. Our detrending technique resulted in a noticeable improvement by reducing the number of false positive and the number of false negative.

1 Introduction

Blood Oxygenation Level-Dependent (BOLD) fMRI uses deoxyhemoglobin as a contrast agent : deoxygenated hemoglobin induces a difference in magnetic susceptibility relative to the surrounding. The cascade of physiological events that trigger the changes in the BOLD signal remains an area of active research [12,2].Unfortunately, changes in the fMRI signal are only of the order of a few percents. The detection of changes in the BOLD signal is further complicated by the presence of a large number of instrumental and physiological noises that contaminate the fMRI signal [5]. Long term physiological drifts and instrumental instability contribute to a systematic increase or decrease in the signal with time. While the exact cause for the drift of the baseline signal is not completely understood [11], this structured trend constitutes a basic hurdle to any statistical analysis of the data. In order to obtain a baseline from which one can estimate the effect of the stimulus it is thus essential to infer and remove the systematic drift, or trend, in the data. In this paper we address the problem of estimating and removing the baseline drift that contaminates the fMRI response to a stimulus. We propose an approach that removes the trend using a multiscale technique.

* This work was supported by a Whitaker Foundation Biomedical Engineering Research Grant.

M.F. Insana, R.M. Leahy (Eds.): IPMI 2001, LNCS 2082, pp. 232–238, 2001.

2 Some Background on Wavelets

We introduce in this section the notations associated with a discrete wavelet transform. These notations will be used in the sequel of the paper. Let $\psi(t)$ be the wavelet, and let $\phi(t)$ be the scaling function associated with a multiresolution analysis [9]. Let $\{h_n\}$ be the lowpass filter, and let $\{g_n\}$ be the high pass filter associated with this wavelet transform. Let $\mathbf{x} = \{x_n\}$, $n = 0, \cdots, N-1$ be a discrete signal. For the simplicity of the presentation we assume that $N = 2^J$. The wavelet coefficients of $\mathbf{x}$ are defined by the following recursions :

$$\begin{array}{ll} sx_k^0 & = x_k \qquad\qquad\qquad k = 0, \cdots, N-1 \\ sx_k^{j+1} & = \sum_n g_{n-2k}\, sx_n^j \quad k = 0, \cdots, 2^{-j-1}N-1 \\ dx_k^{j+1} & = \sum_n h_{n-2k}\, sx_n^j \quad k = 0, \cdots, 2^{-j-1}N-1 \end{array} \tag{1}$$

The wavelet transform $\mathbf{W}$ at scale J is a linear operator that maps $\mathbf{x}$ to $\mathbf{Wx}$ given by :

$$\begin{array}{r} [sx_0^J, dx_0^J,\ dx_0^{J-1}, dx_1^{J-1}, \cdots, dx_0^j, \cdots dx_{2^{-j}N-1}^j, \\ \cdots\cdots\cdots, dx_0^1, \cdots\cdots, dx_{2^{-1}N-1}^1]^t. \end{array} \tag{2}$$

We also require that the wavelet ψ have p vanishing moments. As a consequence, polynomials of degree $p-1$ will have a very sparse representation in such a wavelet basis : all the d_k^j are equal to zero, except for the coefficients located at the border of the dyadic subdivision ($k = 0, 1, 2, 4, \cdots, 2^{J-1}$).

3 Wavelet Estimation of the Drift

While the origin of the baseline drift is not completely understood [6,8,11], a number of artifacts can cause large scale (low frequencies) fluctuations in the signal. Baseline drifts have been described by linear [3,8], and polynomial [4] functions of time. Signal processing techniques such as Kalman filters have recently been proposed [7]. A standard practice consists in approximating trends with polynomials, or a truncated Fourier series [1]. On the one hand, there is no reason to believe that the trend is a periodic function of time that will be well approximated with a few Fourier coefficients. On the other hand, a polynomial provides only a descriptive device. In fact no substantive physical or physiological interpretation can be given to the coefficients. We propose therefore to describe the trend as a superposition of physical and physiological phenomena that occur at different scales.

Model of the drift. We consider the following model for the fMRI time series at a voxel inside the brain :

$$y(t) = \theta(t) + a(t) + n(t) \tag{3}$$

where $\theta(t)$ is the trend, or baseline drift, $a(t)$ is a the response to the stimulus, induced by neuronal activation. This signal will only exist if the voxel is inside

a functionally activated brain area. $n(t)$ is a white noise caused by thermal and quantum noise. An appropriate model for the trend is provided by a linear combination of large scale wavelets :

$$\theta(t) = s_0^J \phi(2^{-J}t) + \sum_{j=J_0}^{J-1} \sum_{k=0}^{2^{-j}N} d_k^j \psi(2^{-j}t - k). \tag{4}$$

This model assumes that all the fine scale coefficients, $d_k^j, \quad 0 \leq j \leq J_0 - 1$, are zero. The smallest scale J_0 characterizes the complexity of the trend.

Estimation of the drift. Let $\mathbf{y} = \{y_n\}, n = 0, .., N-1$ be the time series at a given voxel in the brain. One expands $\mathbf{y}$ into a wavelet basis :

$$\mathbf{W}\mathbf{y} = \left[s_0^J, d_0^J,\ d_0^{J-1}, d_1^{J-1}, \dots, d_0^j, \dots d_{2^{-j}N-1}^j, \dots d_0^1, \dots\dots, d_{2^{-1}N-1}^1 \right] \tag{5}$$

An estimate, $\mathbf{W}\hat{\theta}$, of the wavelet transform of the trend is obtained by taking the first $2^{-J_0+1}N$ terms from the wavelet expansion of $\mathbf{y}$, and setting the other coefficients to zero :

$$\mathbf{W}\theta = \left[s_0^J, d_0^J, \dots, d_0^{J_0}, \dots, d_{2^{-J_0}N-1}^{J_0}, 0, \dots\dots\dots\dots\dots\dots\dots\dots, 0 \right] \tag{6}$$

Alternatively, an estimate $\hat{\mathbf{a}}$ of the detrended time series, $\mathbf{a}$, is obtained by setting the first $2^{-J_0+1}N$ terms in the wavelet expansion (5) to zero, and reconstructing by applying the inverse wavelet transform $\mathbf{W}^{-1}$.

$$\hat{\mathbf{a}} = \mathbf{W}^{-1} \left[0, \dots\dots, 0, d_0^{J_0-1}, .., d_{2^{-J_0+1}N-1}^{J_0-1}, \dots, d_0^1, \dots\dots, d_{2^{-1}N-1}^1 \right] \tag{7}$$

What is the scale of the trend ? The selection of the optimal value of J_0 is performed as follows. We start with $J_0 = J$ which provides the description of the trend with the minimum number of parameters. The significance of $\hat{\mathbf{a}}$ is then tested, and we compute the P-value. We successively test more and more complex models of the trend by decreasing J_0. Because the scale of the trend should be larger than the scale of the stimulus, we stop before J_0 reaches the scale of the stimulus. Finally, one selects that J_0 which provides the smallest P-value. As shown in the experiments, the same value can be used for all activated voxels. This approach guarantees that the detrending algorithm will not increase the P values.

4 Experiments

We illustrate here the principle of the algorithm with some data that demonstrate left posterior temporal lobe activation during auditory comprehension [10]. The study involved several subjects who listened passively to alternating sentences spoken in English (their native language), and Turkish (which they did not understand). Each time series was composed of 28 alternating auditory segments of English and Turkish. Each segment lasted for 6 seconds, and images

were acquired every 1.5 s. There was a delay of 12 seconds from the first image to the onset of the first sentence. TR=1,500, slice thickness=9mm, skip = 2mm, imaging matrix= 128× 64, voxel size = 3.2 × 3.2 × 9 mm. More details about the experiments are available in [10].

Analysis of the detrending performance. We have compared the performance of the detrending algorithm for several values of the scale J_0 of the trend $\theta(t)$. The same value of J_0 was used for all pixels. A time series was extracted from the region of interest (ROI) B in slice 5 (voxel (75,21)), shown in Fig. 2. Figure 1 shows this same time-series with the trend superimposed, for several values of J_0. We note that a piecewise linear trend (such as the one obtained for $J_0 = 8$) fails to track the long term variability of the signal. A Student t-test was designed to compare the signal under the two conditions: English sentences, or Turkish sentences. Pixels with a P-value less than 0.005 were deemed activated, and colored in red in the activation maps.

Result of the first experiment Figure 2 shows the result of the t-test for the slices 4 and 5 after detrending with $J_0 = 4$. The activation maps were thresholded at $P = 0.005$ and are superimposed on the raw EPI data. The left side of the brain is represented on the right side of the image. The maps were generated with two runs of alternating Turkish/English intervals, starting with Turkish. The maps clearly show activated pixels in the left inferior frontal lobe (region A and B). For each slice we selected a region of interest (ROI) that contained strongly activated voxels ($P < 10^{-4}$). The activation in these regions was assumed to be truly caused by the stimulus and not by physiological or random noise. The two ROIs are shown as yellow rectangles, and are pointed at by the arrows A and B in slice 4 and 5 respectively. For each value of the scale of the trend, the performance of the detrending in each ROI was quantified using the following factors : (1) the number of activated voxels inside the ROI, (2) the mean P-value for all the voxels inside the ROI, and (3) the smallest P-value inside the ROI. These numbers are reported in table 1. For both slices the detrending resulted in a noticeable improvement by increasing the number of activated voxels, while decreasing the mean P-value inside the ROIs. The optimal effect was obtained for a scale equal to 4. One notes that as the scale of the trend becomes finer (e.g. $J_0 = 3$), the trend starts tracking the variations in the BOLD signal that are due to the stimulus response, and results in a poorer performance. Because the ROIs in this experiment can be considered as truly activated voxels, this experiments demonstrates that the detrending helps to decrease the number of false positive. Indeed, on can significantly decrease the level of the threshold while keeping the truly activated voxel still activated in the ROIs A and B.

Result of the second experiment A second experiment was conducted with a different data set. Figure 3 shows the result of the t-test for the slices 3 and 4 after detrending with $J_0 = 4$. The activation maps were thresholded at $P = 0.005$ and are superimposed on the raw EPI data. The maps were generated with two runs of alternating English/Turkish intervals, starting with English. The maps show in red activated pixels in the left posterior temporal lobe (regions C and D). For each slice we again selected a region of interest (ROI) that contained

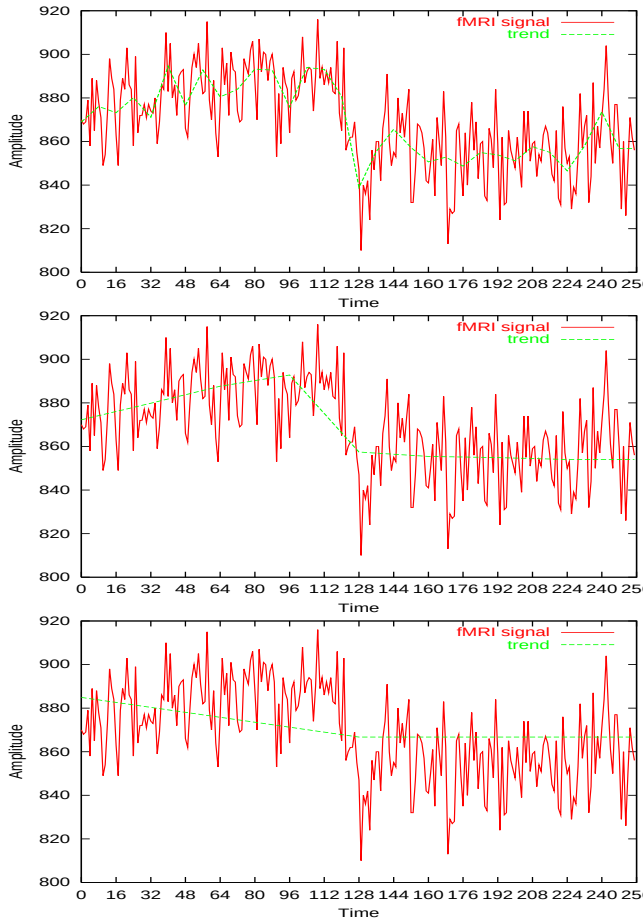

Fig. 1. Trend for different values of the scale J_0. From top to down $J = 4, 6, 8$.

strongly activated voxels ($P < 10^{-3}$). We note that the mean P-value before detrending was not as high as in the previous experiment. The two ROIs are shown as yellow rectangles, and are pointed at by the arrows A and B in slice 4 and 5 respectively. For each value of the scale of the trend, the performance of the detrending in each ROI was quantified using the same factors as in the previous experiments. These numbers are reported in table 2. For both slices the detrending resulted in a noticeable improvement by increasing the number of activated voxels, while keeping the mean P-value inside the ROIs at the same value. The optimal effect was again obtained for a scale equal to 4. This experiment demonstrates that detrending can help reducing the number of false negative : after detrending, there were 4 times more voxels activated in the ROI D, than before detrending.

References

1. T.W. Anderson, *The statistical analysis of time series*, Wiley, 1971.
2. P.A. Bandettini, *The temporal resolution of functional MRI*, Functional MRI (C.T.W. Moonen and P.A. Bandettini, eds.), Springer-Verlag, 1999, pp. 205–220.
3. P.A. Bandettini, A. Jesmanowicz, E.C. Wong, and J.S. Hyde, *Processing strategies for time-course data sets in functional MRI of the human brain*, Magn. Reson. Med. **30** (1993), 161–173.
4. G.H. Glover, *Deconvolution of impulse response in event-related bold fMRI*, NeuroImage (1999), no. 9, 416–429.
5. P. Jezzard, *Physiological noise: strategies for correction*, Functional MRI (C.T.W. Moonen and P.A. Bandettini, eds.), Springer-Verlag, 1999, pp. 173–182.
6. V. Kiviniemi, J. Jauhiainen, O. Tervonen, E. Pääkkö, J. Oikarinen, V. Vainionpää, H. Rantala, and B. Biswal, *Slow vasomotor fluctuation in fMRI of anesthetized child brain*, Magn. Reson. Med. **44** (2000), 373–378.
7. F. Kruggel, D.Y von Cramon, and X. Descombes, *Comparison of filtering methods for fMRI datasets*, NeuroImage (1999), no. 10, 530–543.
8. M.J. Lowe and D.P. Russell, *Treatment of baseline drifts in fMRI time series analysis*, Journal of Computer Assisted Tomography **23(3)** (1999), 463–473.
9. S. Mallat, *A wavelet tour of signal processing*, Academic Press, 1999.
10. M.J. Schlosser, N. Aoyagi, R.K. Fullbright, J.C. Gore, and G. McCarthy, *Functional MRI studies of auditory comprehension*, Human Brain Mapping **6** (1998), 1–13.
11. A.M. Smith, B.K. Lewis, U.E. Ruttimann, F.Q. Ye, T.M. Sinnwell, Y. Yang, J. H. Duyn, and J.A. Frank, *Investigation of low frequency drift in fMRI signal*, NeuroImage (1999), no. 9(5), 526–533.
12. I. Vanzetta and A. Grinvald, *Increased cortical oxidative metabolism due to sensory stimulation: implications for functional brain imaging*, Science **286** (1999), 1555–8.

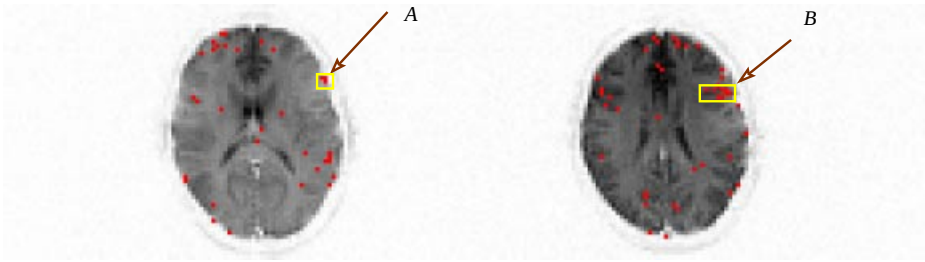

Fig. 2. Turkish-English. Left : slice 4. Right : slice 5. Activation map ($p = 0.005$). The scale of the trend was $J_0 = 4$.

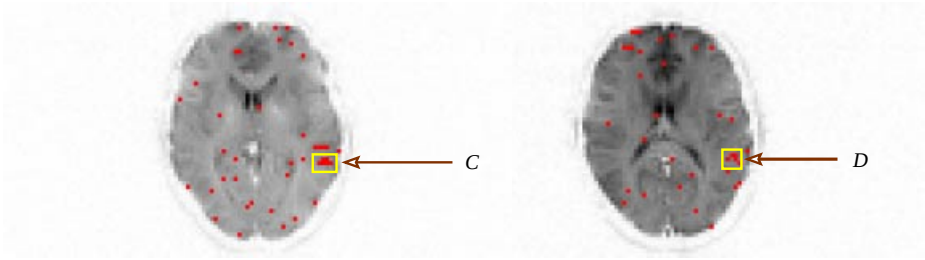

Fig. 3. English-Turkish. Left : slice 3. Right : slice 4. Activation map ($p = 0.005$). The scale of the trend was $J_0 = 4$.

Table 1. Turkish-English. Left : slice 4, ROI A (4 voxels). Right: slice 5, ROI B (6 voxels).

Scale J_0	# activated voxels	mean P-value	minimum P-value
3	1	6.90e-05	6.90e-05
4	3	1.36e-05	4.57e-06
5	3	1.56e-04	8.16e-06
6	3	1.83e-04	8.00e-06
7	3	7.27e-04	1.07e-05
8	2	6.41e-05	6.06e-05
No trend	2	1.29e-04	7.10e-05

Scale J_0	# activated voxels	mean P-value	minimum P-value
3	3	2.20e-05	1.17e-05
4	4	1.82e-04	3.33e-08
5	4	2.47e-04	1.03e-07
6	4	3.15e-04	2.09e-07
7	4	3.43e-04	2.38e-07
8	3	9.10e-04	5.04e-07
No trend	2	1.20e-03	8.88e-07

Table 2. English-Turkish. Left : slice 3, ROI C (8 voxels). Right : slice 4, ROI D (9 voxels).

Scale J_0	# activated voxels	mean P-value	minimum P-value
3	4	2.10e-03	8.65e-05
4	6	1.11e-03	4.20e-06
5	5	8.17e-04	1.39e-05
6	6	1.81e-03	1.81e-05
7	5	1.39e-03	3.25e-05
8	5	1.31e-03	6.32e-05
No trend	4	1.20e-03	3.75e-04

Scale J_0	# activated voxels	mean P-value	minimum P-value
3	1	3.31e-03	3.31e-03
4	4	6.09e-04	3.11e-05
5	4	8.51e-04	4.70e-05
6	4	1.15e-03	7.60e-05
7	4	1.49e-03	1.81e-04
8	4	1.50e-03	1.39e-04
No trend	1	1.89e-03	1.89e-03